IEEE Access
Multidisciplinary | Rapid Review | Open Access Journal

Received 9 March 2023, accepted 31 March 2023, date of publication 12 April 2023, date of current version 21 April 2023.

Digital Object Identifier 10.1109/ACCESS.2023.3266558

RESEARCH ARTICLE

MM-Wave High Isolated Dual Polarized Dielectric Resonator Antenna for In-Band Full-Duplex Systems

MOHAMMAD ABEDIAN[1], (Member, IEEE), MOHSEN KHALILY[1], (Senior Member, IEEE), PEI XIAO[1], (Senior Member, IEEE), FAN WANG[2], RAHIM TAFAZOLLI[1], (Senior Member, IEEE), AND AHMED A. KISHK[3], (Life Fellow, IEEE)

[1]Institute for Communication Systems (ICS), Home of the 5G & 6G Innovation Centres, University of Surrey, GU2 7XH Guildford, U.K.
[2]Wireless Technology Laboratory, Huawei Technologies Company Ltd., Shanghai 518129, China
[3]Department of Electrical and Computer Engineering, Concordia University, Montreal, QC H3G 2W1, Canada

Corresponding author: Mohsen Khalily (m.khalily@surrey.ac.uk)

ABSTRACT A novel high-isolation dual-polarized in-band full-duplex (IBFD) dielectric resonator antenna (DRA) for satellite communications using a decoupling structure is proposed. Good isolation between transmit and receive ports is achieved by placing two identical linearly polarized resonators orthogonal to each other. Each resonator consists of a main rectangular dielectric resonator of the dielectric constant of 10 and is loaded by a thin dielectric slab of lower permittivity of 5 to broaden the matching bandwidth further. The isolation is further improved by loading an absorber and etching several slots in the ground plane. Finally, the proposed DRA is fabricated and measured to validate the concepts. Measurement results show high isolation of more than 50 dB over the desired operating bandwidth from 23.04 GHz to 24.08 GHz (ka-band) with a peak gain of about 8.93 dBi and 8.09 dBi for Port 1 and Port 2, respectively. In addition, the proposed IBFD DRA provides 11.87 GHz and 4.84 GHz isolation bandwidths over 25 dB and 30 dB, respectively, making it a potential candidate for mm-wave terrestrial applications.

INDEX TERMS Dielectric resonator antenna, dual-polarization, in-band full-duplex.

I. INTRODUCTION

In recent years, deployable electromagnetic spectra have been highly demanded by dramatically increasing data traffic in wireless communication. As an emerging new transmission technology, in-band full-duplex (IBFD) communication, which simultaneously transmits (Tx) and receives (Rx) signals over the same frequency band, has attracted immense attention as a promising technique to increase spectrum efficiency with the potential to double the channel capacity compared to that of a time/frequency division method [1], [2]. However, practically, in the IBFD system, due to the existence of high self-interference (SI) in the system, where the transmitted signal leaks to the Rx side, high isolation (as much as 110 dB) between Tx and Rx channels is required [3].

The associate editor coordinating the review of this manuscript and approving it for publication was Davide Ramaccia.

In order to minimize the coupling in a full-duplex system, including antenna, RF, baseband, and digital domains, multilayer self-interference cancellation (SIC) approaches are needed correspo0nding to antenna isolation, active/passive analogue cancellation circuits, and digital cancellation algorithms. The main bottleneck problems with the current IBFD system design include bandwidth limitation imposed by the RF self-interference cancellation circuits and implementation complexity, and large insertion loss associated with RF SIC circuits. As such, achieving high isolation in the antenna domain relieves the burden placed on other layers and helps mitigate the overall complexity of a simultaneously transmits and receives (STAR) transceiver [4].

A plethora of full-duplex (FD) antennas with high isolation, including microstrip, cavity, and slot antennas, have been reported in the literature [5], [6], [7], [8], [9], [10], [11], [12], [13], [14], [15], [16], [17], [18], [19], [20], [21], [22],

[23], [24], [25], [26]. Nevertheless, most of these designs operate at frequency bands below 20 GHz. On the other hand, there have been increasing full-duplex applications for millimetre-wave (mm-wave) transmissions for high data rate communications in the past decade. However, the inherent problems with mm-wave, such as high path loss, necessitate high gain antenna design [8]. Various techniques exist to improve the isolation between the TX and the Rx antennas [10], [11], [7], [12], [13], [14], [15], [16], [17], [18], [19], [20], [21], [22], [23], [24], [25]. Generally, these methods are divided into several main categories, such as physical separation between Tx and Rx apertures [9], [10], utilizing polarization multiplexing [11], [7], [12], [13], employing near-field cancellation [14], [15], [16], and implementing circulators [17], [18], [19]. Finally, the decoupling technique suppresses the self-interference caused by the electromagnetic coupling between the Tx and Rx antennas [20], [21], [22], [23], [24], [25]. For example, in [22], a radiating element is applied between Rx and Tx antennas, coupling power from the Tx antenna. It is orthogonally polarized and re-radiates the power to minimize the original field around the Rx antenna. Furthermore, in [24], a power distributing duplex network is employed to obtain high isolation of about 45 dB between the two input ports. As for the one presented in [25], the electromagnetic bandgap (EBG) structure is inserted between two closely located monopole antennas to improve isolation. As a result, the achieved isolation is up to 50 dB in 110 MHz bandwidth at around 2.5 GHz. However, generally speaking, most of the works, as mentioned earlier, suffer from a high cost, a large antenna dimension, narrow bandwidth, low radiation efficiency, or a complex structure.

Here, we propose a high isolation dual-polarized IBFD dielectric resonator antenna (DRA) at mm-wave with high radiation efficiency for the first time that can be extended to an IBFD array DRA achieving desirable gain for satellite communications. DRAs have been extensively studied in past decades because of their remarkable features, such as low loss, no surface wave, high radiation efficiency, various excitation mechanisms, and geometrical flexibility [26], [27]. In addition, the 3-D geometry of DRAs offers a higher degree of flexibility over microstrip antennas that suffer from narrow bandwidth and low radiation efficiency [28]. In addition, we use the feature of low coupling between DRAs of high order odd index in the z-direction [29]. High isolation better than 50 dB is realized by loading a thin rectangular dielectric resonator (DR) attached to two strips at the top and the bottom, applying a vertical strip connected to both the ground plane and thin DR, and etching several slots in the ground plane. The configuration and the design procedure, a numerical study on designing IBFD DRA, the effects of loading thin DRs, the impact of adding decoupling structure and etching the slots in the ground plane, and the measurement results on fabricated prototype are discussed in the following sections.

II. ANTENNA CONFIGURATION AND PHYSICAL WORKING MECHANISM

A rectangular DR (RDR) offers more design parameters, such as two different aspect ratios (width/length and height/length) in a desired resonant frequency compared to the spherical and cylindrical ones. Parallelly, in IBFD antenna design, although there are various techniques to achieve 50 dB antenna isolation, the supported bandwidth is narrow and suffers from the large size, complexity, or dissimilar transmit/receive radiation.

The evolution of the proposed high-isolation dual-polarized IBFD DRA is demonstrated in Fig. 1. Fig. 1(a) shows the initial design of the proposed antenna, including two identical RDRs (DR_1) with the same dimensions $a_1 \times b_1 \times h_1$ and permittivity of $\varepsilon_{DR_1} = 10$ supported by a grounded $23(x-axis)mm \times 14.1(y-axis)mm$ Rogers RT5880 substrate with a permittivity of $\varepsilon_s = 2.2$ and a thickness of $s = 0.127\ mm$, where maximum isolation of about 43 dB is achieved. The RDRs are excited by a microstrip feed line through a rectangular metal strip $l_5 \times w_6$. Then, another two small identical RDRs (DR_2) with the exact dimensions of $a_3 \times b_3 \times h_3$ and permittivity of $\varepsilon_{DR_2} = 5$ are attached to the previous RDRs with a reducing length from $4mmto3.5\ mm$ to improve the impedance matching (please see Fig. 1(c)), denoted as Antenna I. To further improve the isolation, two slots with $l_3 \times w_2$ are etched in the ground plane in the transverse direction of each microstrip feed line (please see Fig. 1(d)), denoted as Antenna II. Finally, a new decoupling structure, including a vertical and two horizontal strip patches, a slot in the ground plane, and a thin RDR (DR_3) with a dimension of $a_4 \times b_4 \times h_4$ and a dielectric constant of $\varepsilon_{DR_m} = 10$, is introduced to enhance the isolation bandwidth (please see Fig. 1(e)), denoted as Antenna III. All DRs have a relative loss tangent $tan\,\delta = 1.54 \times 10^{-5}$.

In this work, CST Microwave Studio 2021 is employed to analyze and optimize the proposed IBFD DRA. The ultimate aim of this design is to propose a new dual-polarized antenna with high isolation to realize full-duplex radio transmissions over satellites considering two crucial parameters; antenna efficiency and isolation. The main contribution of this work is to propose a dual-polarized DRA with 50 dB wide isolation bandwidth between the Tx and Rx ports and efficiency higher than 93% at the Ka-band, which is the first of its kind. This section describes the working principle of the proposed IBDF DRA and the physical mechanisms, which include three steps as follows:

I Loading a small rectangular dielectric slab with a dielectric constant of 5 to improve the maximum isolation from 42 dB to 55 dB with an isolation bandwidth of 170 MHz over 50 dB.
II Adding slots on top of the feed lines improves the isolation between two ports from 55 to 62 dB and enhances the bandwidth from 170 MHz to 270 MHz for the 50 dB threshold.

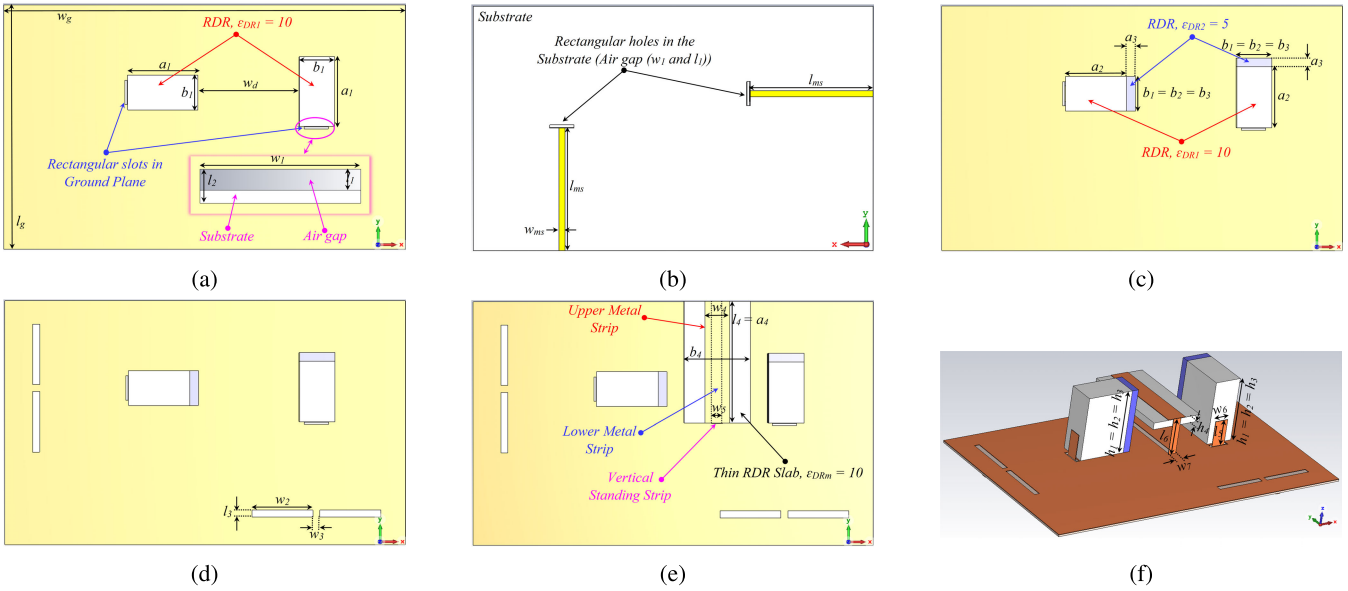

FIGURE 1. Evolution of the proposed IBFD DRA: (a) initial structure of IBFD DRA, (b) back view of the proposed antenna(microstrip feed lines), (c) adding two small RDRs with low permittivity to the initial structure, forming Antenna I, (d) applying narrow slots in the ground plane of Antenna I, denoting Antenna II, (e) adding an absorber with an opening slot beneath it to the Antenna II, namely Antenna III, and (f) 3D view of the proposed antenna (Antenna III). ($l_g = 14.1$, $w_g = 23$, $l_1 = 0.185$, $l_2 = 0.3$, $l_3 = 0.4$, $l_5 = 1.9$, $l_6 = 2.7$, $w_d = 5.8$, $w_1 = 1.4$, $w_2 = 3.5$, $w_3 = 0.4$, $w_4 = 1.4$, $w_5 = w_7 = 0.5$, $w_6 = 1$, $l_{ms} = 0.7.1$, $w_{ms} = 0.36$, $a_1 = 4$, $b_1 = b_2 = b_3 = 2$, $h_1 = h_2 = h_3 = 4.7$, $a_2 = 3.5$, $a_3 = 0.5$, $a_4 = 7$, $b_4 = 3.8$, $h_4 = 0.5$, $\varepsilon_{DR_1} = \varepsilon_{DRm} = 10$, $\varepsilon_{DR_2} = 5$, $\varepsilon_s = 2.2$, $s = 0.127$. *Unit* : *mm*).

III Applying a decoupling structure remarkably improves the isolation bandwidth from 270 MHz to 1090 MHz over 50 dB with peak isolation of 70 dB.

III. IBFD DRA DESIGN ANALYSIS

As shown in Fig. 1(a), the initial dual-polarized IBFD DRA is realized by two RDRs with equal dimensions $a_1 \times b_1 \times h_1$ (a_1 and $h_1 \gg b_1$) orthogonally excited by vertical metal strips attached to the DRA side wall and connected to microstrip feed lines (in the bottom side of a dielectric substrate) through a narrow rectangular hole to realize the dual-polarized performance. The distance between DRs (wall-to-wall) is defined as $w_d = 0.58\lambda$. The proposed antenna system has two ports: one supports TE^x_{mnp} mode for Tx and the other one supports TE^y_{mnp} mode for Rx. Both input and output ports of the system can operate simultaneously. The dielectric waveguide model (DWM) equations are used to predict the resonant frequency f_r of TE_{mnp} modes excited inside the proposed DRA [30]:

$$f_r = \frac{1}{2\,\pi\,\sqrt{\varepsilon_{DR}}}\sqrt{k_x^2 + k_y^2 + k_z^2} \tag{1}$$

where k_x, $k_y = n\pi/a$, and $k_z = p\pi/2h$ are the mode wave numbers within the RDR. The following characteristic Equation should be solved for k_x for each mode index m for a variable k_0

$$k_x tan(\frac{bk_x - (m-1)\pi}{2}) = \sqrt{(\varepsilon_{DR} - 1)k_0^2 - k_x^2} \tag{2}$$

The solution for each m determines the other mode indices n and p in the y- and z-directions.

In order to improve the impedance bandwidth, a small rectangular dielectric slab with dimension $a_3 \times b_3 \times h_3$ and dielectric constant $\varepsilon_{DR_2} = 5$ is added to each previous RDR with reduced length to $a_2 \times b_2 \times h_2$ ($a_2 = 3.5\ mm$; $b_1 = b_2$, $h_1 = h_2$) (please see Fig. 1 (c)), namely as Antenna I. It is noted that the new resonant frequency can be calculated by substituting ε_{DR_1} with ε_{eff} (effective dielectric constant) in Equation (2) [27], where

$$\varepsilon_{eff} = \frac{a_1 + a_2}{\frac{a_1}{\varepsilon_{DR_1}} + \frac{a_2}{\varepsilon_{DR_2}}} \tag{3}$$

Figure 2 illustrates the simulated s-parameters of the initial structure of IBFD DRA and Antenna I (please see Fig. 2 (a) and (b)) and E-field distribution inside the DRs (please see Fig. 2 (c)) for the Antenna I at 23.5 GHz. It is observed from Fig. 2 (a) that the RDRA provides a wide impedance bandwidth of about 60% (Port 1) and 58% (Port 2), and exciting resonant modes across the operating frequency resembles TE_{111}, TE_{113}, and TE_{115} modes. Maximum isolation of 43 dB at 23.5 GHz is obtained, corresponding to TE^x_{113} and TE^y_{113} modes (please see Fig. 2 (c)). In the next step (refer to Fig. 1(c)), by loading two thin RDRs ($\varepsilon_{DR_2} = 5$), the impedance matching and the mutual coupling between two orthogonal resonators is improved due to decreasing the Q-factor of the resonators, resulting in better matching with enhanced isolation to a maximum of about 55 dB, as shown in Fig. 2 (a) and (b).

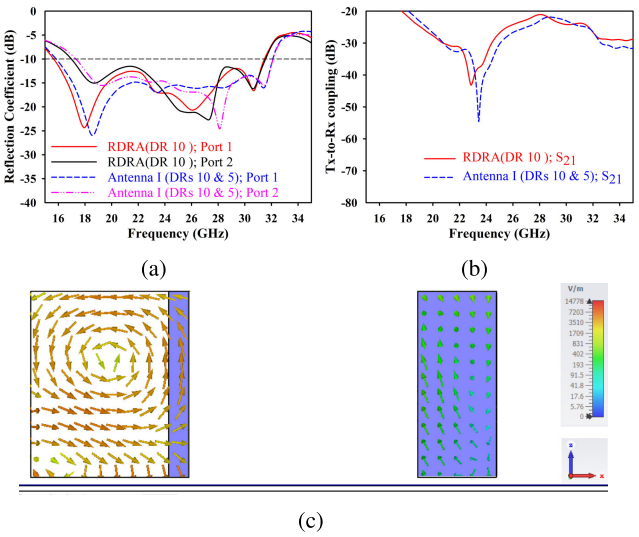

FIGURE 2. Simulated S-parameters of the initial structure of IBFD DRA and Antenna I and E-field distribution inside the RDRs for Antenna I. (a) $|S_{11}|$ and $|S_{22}|$, (b) $|S_{12}| = |S_{21}|$, and (c) TE^{y}_{113} mode at 23.5 GHz (left resonator).

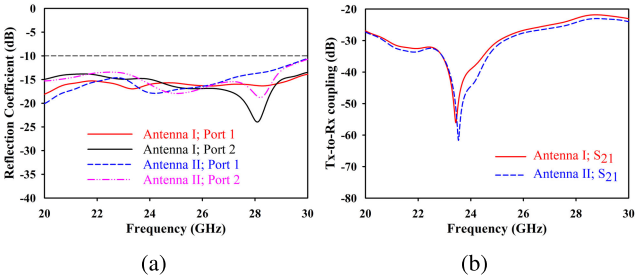

FIGURE 3. Simulated S-parameters of Antenna I and Antenna II (added slots). (a) $|S_{11}|$ and $|S_{22}|$, (b) $|S_{12}| = |S_{21}|$.

ADDING DECOUPLING STRUCTURE TO IMPROVE THE ISOLATION

As shown in Fig. 1 (d), four identical slots with key parameters of $l_3 \times w_2$ are etched in the ground plane on top of the feed lines to improve the isolation between two ports, namely Antenna II.

Figure 3 shows the simulated S-parameters of the IBFD DRA with and without the slots. By etching four equal rectangular slots, the isolation between Tx and Rx channels is enhanced to 62 dB with an isolation bandwidth ranging from 23.41 GHz to 23.68 GHz over 50 dB. In this way, the slots act as matching stubs. Consequently, the coupling current on the ground plane is reduced by generating opposite currents around the slots, resulting in improved isolation.

Finally, for further minimizing the mutual coupling and enhancing the isolation bandwidth, a decoupling structure, including a thin RDR (DRm) slab with dimensions $a_4 \times b_4 \times h_4$ and dielectric constant $\varepsilon_{DR_m} = 10$, placed between two parallel metal strips at the top and the bottom, all connected to a vertical standing strip, is introduced, namely Antenna III. Fig. 4 shows the exploded view of the proposed

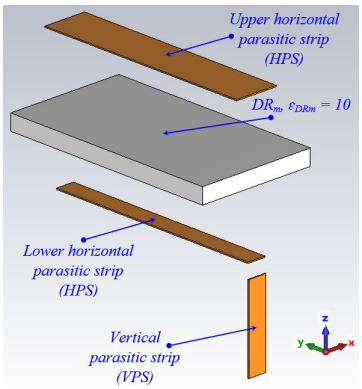

FIGURE 4. Exploded view of the proposed absorber.

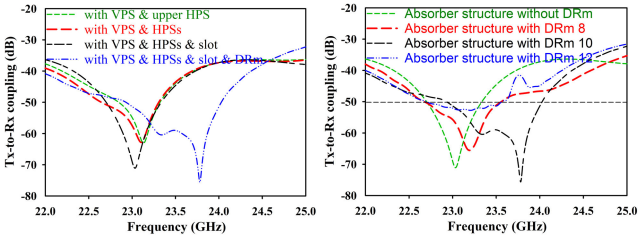

FIGURE 5. Simulated Tx-to-Rx coupling of the proposed antenna (a) with and without each element of decoupling structure separately and (b) with different DRm permittivity.

absorber, shedding light on the proposed absorber design consideration. First, a vertical standing strip is connected to the ground plane at the bottom and a parasitic strip at the top to improve the isolation bandwidth from 270 MHz to 475 MHz over 50 dB. Then, a second parasitic strip, parallel to the first one by 0.5 *mm* distance in the *z*-direction, is applied to further enhance the isolation bandwidth by 210 MHz (from 475 MHz to 685 MHz over 50 dB). A 0.4 (*x*-axis) *mm* × 7 (*y*-axis) *mm* slot is etched on the ground plane to increase the isolation by 10 dB, from 63 dB to 73 dB. Finally, a dielectric slab with a permittivity of 10 and thickness of 0.5 *mm* is horizontally placed between two parallel strips to improve the isolation bandwidth further, shown in Fig. 5 (a). Fig. 5 (b) illustrates the simulated Tx-to-Rx coupling of the proposed antenna with different values of DR permittivity $\varepsilon_{DR_m} = 0$, 8, 10, and 12. According to the figure, a wider isolation bandwidth is achieved by using a permittivity of $\varepsilon_{DR_m} = 10$ to design the proposed absorber. The effect of the decoupling structure on the antenna performance is exhibited in Fig. 6. It is observed from Fig.6 (b) that by implementing the decoupling structure between two resonators, the isolation bandwidth is remarkably improved from 240*MHz* in Antenna II to 1090 MHz in Antenna III. The simulated electric field vectors on different surfaces of the DRs and current distribution for Antenna III at 23.5 GHz are illustrated in Fig. 6 (c), (d), and (e), respectively. By applying the proposed decoupling structure, the EM waves between two resonators are absorbed by DRm. Consequently, a sharp contrast between

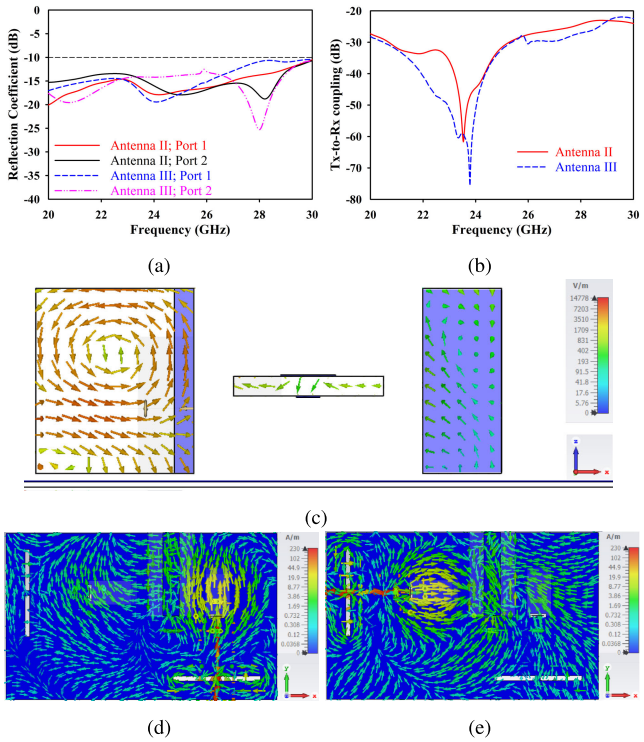

FIGURE 6. Simulated S-parameters of the Antenna II and the Antenna III and E-field and current distributions for Antenna III. (a) reflection coefficient, (b) Tx-to-Rx coupling, (c) modes inside each DR block, and surface current distributions for the Antenna III at 23.5 GHz when (d) Port 1 and (e) Port 2 are excited.

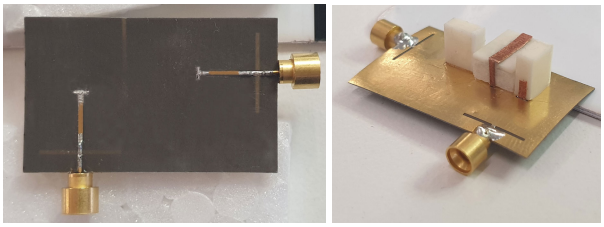

FIGURE 7. The prototype of the proposed IBFD dual-polarized DRA. (a) back view and (b) 3D view.

the current distributions on the left and right side of the decoupling elements leads to significantly enhanced isolation bandwidth between the Tx and Rx ports.

IV. EXPERIMENTAL RESULTS

As illustrated in Fig. 7, a prototype of the proposed IBDF dual-polarized DRA is simulated, fabricated, assembled, and measured to verify the performance of the proposed antenna. A ROHACELL®. HF Foam ($\varepsilon_{ro} = 1.04$) is glued beneath the DRm using RTV silicone adhesive ($\varepsilon_g =\approx 3$) to assemble the decoupling elements between the Rx and Tx resonators.

S-PARAMETER MEASUREMENT

The simulated and measured S-parameters of the proposed IBDF dual-polarized DRA are depicted in Fig. 8, representing a close agreement between the simulated and measured

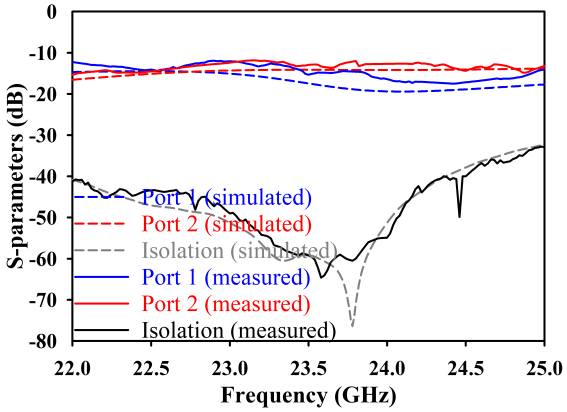

FIGURE 8. Simulated and measured S-parameters of the proposed IBFD dual-polarized DRA.

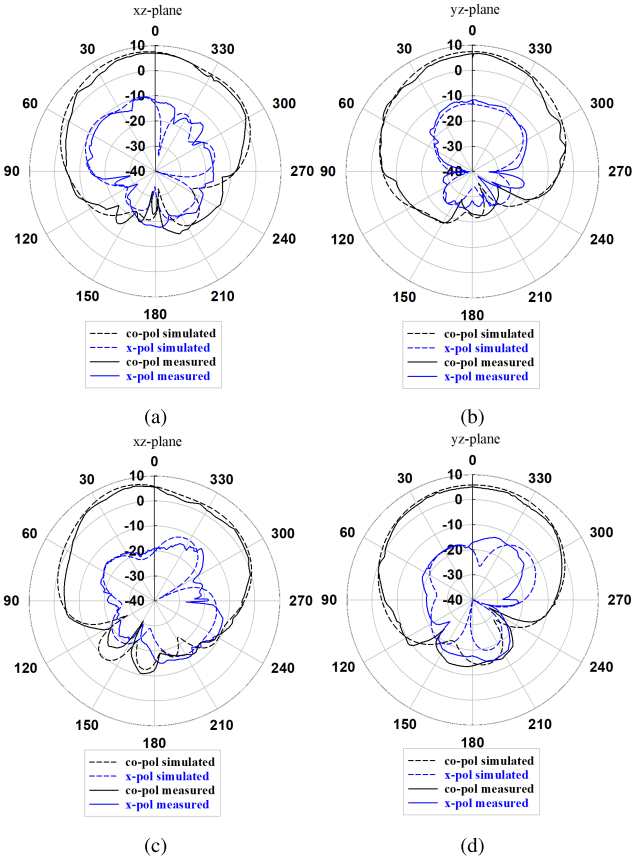

FIGURE 9. Simulated and measured far-field radiation patterns of the proposed IBFD DRA in *xz*-plane ($\phi = 0°$) and *yz*-plane ($\phi = 90°$) at 23.5 GHz; (a) Port 1 and (b) Port 2.

results except for a slight discrepancy caused by the fabrication errors and manually assembling imperfection. The proposed IBFD DRA provides a perfectly overlapping ultra-wide impedance bandwidth for Ports 1 and 2. As shown in Fig. 8, the proposed DRA provides isolation higher than 50 dB in the desired bands, ranging from 22.93 GHz to 24.02 GHz and 23.04 GHz to 24.08 GHz for the simulation and the

TABLE 1. Comparison with IBFD Antennas in the literature.

Ref.	f_c (GHz)	BW (GHz)	Dimensions(λ^3)	Isolation(dB)	Tx/Rx peak gain	G/V	Efficiency
[5]	3.57	3.35-3.8	0.45×0.2×0.04	$\geqslant$ 43	2.8/2.8	777	$\geqslant$70
[12]	2.45	2.4-2.62	1.17×1.69×0.05	$\geqslant$ 35.9	8.02	81	NA
[18]	2.55	2.4-2.7	0.98×0.98×0.15	40	1.8/3.3	22	NA
[21]	2.4	2.3-2.6	$\gg$ 3.68×1.63	$\geqslant$ 45	3	$\ll$ 0.5	$\geqslant$90
[22]	6.29	6.24-6.34	0.63×0.63×0.08	$\geqslant$ 25	3.87/7.58	236	$\geqslant$ 75
[23]	2.45	2.42-2.47	0.54×0.18×0.06	30	-1.6	274	$\leqslant$ 60
[24]	5.8	5.62-6.11	1.2×1.07×0.578	50	5.3/6	8	NA
This work	**23.56**	**23.04-24.08**	**1.8 × 1.1 × 0.39**	**$\geqslant$ 50**	**8.93/8.09**	**12**	**$\geqslant$ 93**

f_c: center frequency, BW: overlapping bandwidth, and G/V: gain to volume.

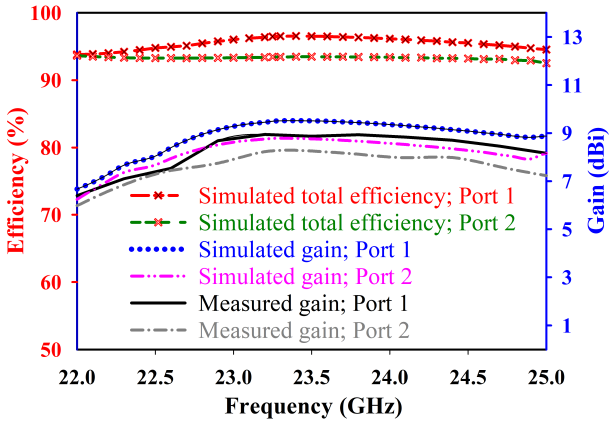

FIGURE 10. Simulated total efficiency and measured gain of the proposed antenna.

measurement. It is noted that the maximum measured and simulated isolation within the studied band are up to 65.21 dB at 23.58 GHz and 76.43 dB at 23.78 GHz, respectively.

A. FAR-FIELD MEASUREMENT

Figure 9 illustrates the simulated and the measured far-field radiation patterns of the proposed IBFD DRA in the *xz*-plane ($\phi = 0°$) and *yz*-plane ($\phi = 90°$) at 23.5 GHz. It is observed that the simulated and measured radiation patterns are in good agreement, where the proposed DRA's radiation patterns remain stable within the desired operating band, and the difference between Co- and cross-polarization radiation levels is more than 21 dB confirming the purity of the radiation. It is worth mentioning that the proposed antenna provides a total efficiency higher than 93% in the desired frequency bands (23.04 GHz to 24.08 GHz) with a maximum gain corresponding to Port 1 and Port 2 of about 9.36 dBi and 8.57 dBi for simulation, and 8.93 dBi and 8.09 dBi for measurements, respectively, shown in Fig. 10.

B. COMPARISON WITH THE LITERATURE

The state-of-the-art high isolation antennas are summarized and listed in Table 1 for comparisons in terms of the critical performance metrics. It is found that the proposed antenna offers higher isolation with higher gain and efficiency using a simple single-substrate design and feeding structure. Wang et al. [12] proposed a reflective terminal approach to improve isolation. Compared to [12], where double substrate topology is used, the proposed design offers higher isolation with a simple single substrate design. Moreover, the antennas in [17], [20], and [22] suffer poor isolation performances. The antennas in [5] and [21] have high isolation but with a reduced low gain. In the design in [23], although high isolation of up to 50 dB is achieved, the employed structure cannot be extended to mm-wave and suffer from low efficiency.

V. CONCLUSION

A dual-polarized in-band full-duplex dielectric resonator antenna has been presented. Two dielectric resonators with different dielectric constants were employed to improve the impedance bandwidth with better isolation. A decoupling element was incorporated to further isolation improvement, including three metal strips and a dielectric resonator to provide a high isolation bandwidth. The proposed antenna was fabricated, assembled, and measured. The measured results have demonstrated high isolation, within frequency ranging from 23.04 to 24.08. The maximum realized gain of 8.93 dBi and 8.09 dBi for Ports 1 and 2, respectively. The proposed IBFD dual-polarized DRA offers a high gain antenna with high isolation, which is a potential candidate for the in-band full-duplex applications at mm-wave frequencies, especially for ka-band satellite communications. Furthermore, the proposed antenna provides 11.87 GHz and 4.84 GHz isolation bandwidths over 25 dB and 30 dB, respectively, which could be utilized for mm-wave terrestrial applications.

REFERENCES

[1] D. Korpi, M. Heino, C. Icheln, K. Haneda, and M. Valkama, "Compact inband full-duplex relays with beyond 100 dB self-interference suppression: Enabling techniques and field measurements," *IEEE Trans. Antennas Propag.*, vol. 65, no. 2, pp. 960–965, Feb. 2017.

[2] M. Tsunezawa, K. Takahashi, N. Honma, K. Murata, and K. Nishimori, "Antenna arrangement suitable for full-duplex MIMO," *IEEE Trans. Antennas Propag.*, vol. 65, no. 6, pp. 2966–2974, Jun. 2017.

[3] A. Sabharwal, P. Schniter, D. Guo, D. W. Bliss, S. Rangarajan, and R. Wichman, "In-band full-duplex wireless: Challenges and opportunities," *IEEE J. Sel. Areas Commun.*, vol. 32, no. 9, pp. 1637–1652, Sep. 2014.

[4] K. E. Kolodziej, B. T. Perry, and J. S. Herd, "In-band full-duplex technology: Techniques and systems survey," *IEEE Trans. Microw. Theory Techn.*, vol. 67, no. 7, pp. 3025–3041, Jul. 2019.

[5] Z. Wang, T. Liang, and Y. Dong, "Compact in-band full duplexing antenna for sub-6 GHz 5G applications," *IEEE Antennas Wireless Propag. Lett.*, vol. 20, no. 5, pp. 683–687, May 2021.

[6] Y. He and Y. Li, "Compact co-linearly polarized microstrip antenna with fence-strip resonator loading for in-band full-duplex systems," *IEEE Trans. Antennas Propag.*, vol. 69, no. 11, pp. 7125–7133, Nov. 2021.

[7] Y.-M. Zhang and J.-L. Li, "Differential-series-fed dual-polarized traveling-wave array for full-duplex applications," *IEEE Trans. Antennas Propag.*, vol. 68, no. 5, pp. 4097–4102, May 2020.
[8] D. Lockie and D. Peck, "High-data-rate millimeter-wave radios," *IEEE Microw. Mag.*, vol. 10, no. 5, pp. 75–83, Aug. 2009.
[9] P. V. Prasannakumar, M. A. Elmansouri, and D. S. Filipović, "Wideband decoupling techniques for dual-polarized bi-static simultaneous transmit and receive antenna subsystem," *IEEE Trans. Antennas Propag.*, vol. 65, no. 10, pp. 4991–5001, Oct. 2017.
[10] O. N. Alrabadi, A. D. Tatomirescu, M. B. Knudsen, M. Pelosi, and G. F. Pedersen, "Breaking the transmitter–receiver isolation barrier in mobile handsets with spatial duplexing," *IEEE Trans. Antennas Propag.*, vol. 61, no. 4, pp. 2241–2251, Apr. 2013.
[11] H. Nawaz and I. Tekin, "Double-differential-fed, dual-polarized patch antenna With 90 dB interport RF isolation for a 2.4 GHz in-band full-duplex transceiver," *IEEE Antenna Wireless Propag. Lett.*, vol. 17, no. 2, pp. 287–290, Feb. 2018.
[12] X. Wang, W. Che, W. Yang, W. Feng, and L. Gu, "Self-interference cancellation antenna using auxiliary port reflection for full-duplex application," *IEEE Antennas Wireless Compon. Lett.*, vol. 16, pp. 2873–2876, 2017.
[13] Y. Zhang and J. Li, "A dual-polarized antenna array with enhanced interport isolation for far-field wireless data and power transfer," *IEEE Trans. Veh. Technol.*, vol. 67, no. 11, pp. 10258–10267, Nov. 2018.
[14] A. J. Fenn, P. T. Hurst, J. S. Herd, K. E. Kolodziej, L. I. Parad, and H. Steyskal, "Simultaneous transmit and receive antenna system," U.S. Patent 8 749 441 B2, Jun. 10, 2014.
[15] D. Wu, Y. Zang, H. Luyen, M. Li, and N. Behdad, "A compact, low-profile simultaneous transmit and receive antenna with monopole-like radiation characteristics," *IEEE Antennas Wireless Propag. Lett.*, vol. 18, no. 4, pp. 611–615, Apr. 2019.
[16] R. Lian, T. Shih, Y. Yin, and N. Behdad, "A high-isolation, ultrawideband simultaneous transmit and receive antenna with monopole-like radiation characteristics," *IEEE Trans. Antennas Propag.*, vol. 66, no. 2, pp. 1002–1007, Feb. 2018.
[17] M. R. Nikkhah, J. Wu, H. Luyen, and N. Behdad, "A concurrently dual-polarized, simultaneous transmit and receive (STAR) antenna," *IEEE Trans. Antennas Propag.*, vol. 68, no. 8, pp. 5935–5944, Aug. 2020.
[18] A. H. Abdelrahman and D. S. Filipovic, "Antenna system for full-duplex operation of handheld radios," *IEEE Trans. Antennas Propag.*, vol. 67, no. 1, pp. 522–530, Jan. 2019.
[19] Z. Zhou, Y. Li, J. Hu, Y. He, Z. Zhang, and P.-Y. Chen, "Monostatic copolarized simultaneous transmit and receive (STAR) antenna by integrated single-layer design," *IEEE Antennas Wireless Propag. Lett.*, vol. 18, no. 3, pp. 472–476, Mar. 2019.
[20] K. Iwamoto, M. Heino, K. Haneda, and H. Morikawa, "Design of an antenna decoupling structure for an inband full-duplex collinear dipole array," *IEEE Trans. Antennas Propag.*, vol. 66, no. 7, pp. 3763–3768, Jul. 2018.
[21] W. Zhang, J. Hu, Y. Li, and Z. Zhang, "Design of a stacked co-polarized full-duplex antenna with broadside radiation," *IEEE Trans. Antennas Propag.*, vol. 69, no. 11, pp. 7111–7118, Nov. 2021.
[22] S. N. Venkatasubramanian, L. Li, A. Lehtovuori, C. Icheln, and K. Haneda, "Impact of using resistive elements for wideband isolation improvement," *IEEE Trans. Antennas Propag.*, vol. 65, no. 1, pp. 52–62, Jan. 2017.
[23] N.-A. Nguyen, V. H. Le, N. Nguyen-Trong, M. Radfar, A. Ebrahimi, K. Phan, and A. Desai, "Dual-polarized slot antenna for full-duplex systems with high isolation," *IEEE Trans. Antennas Propag.*, vol. 69, no. 11, pp. 7119–7124, Nov. 2021.
[24] X.-J. Lin, Z.-M. Xie, and P.-S. Zhang, "Integrated filtering microstrip duplex antenna array with high isolation," *Int. J. Antennas Propag.*, vol. 2017, pp. 1–8, Jan. 2017.
[25] J.-Y. Lee, S.-H. Kim, and J.-H. Jang, "Reduction of mutual coupling in planar multiple antenna by using 1-D EBG and SRR structures," *IEEE Trans. Antennas Propag.*, vol. 63, no. 9, pp. 4194–4198, Sep. 2015.
[26] K. M. Luk and K. W. Leung, *Dielectric Resonator Antennas*. Baldock, U.K.: Research Studies Press, 2003.
[27] R. K. Mongia and A. Ittipiboon, "Theoretical and experimental investigations on rectangular dielectric resonator antennas," *IEEE Antennas Propag.*, vol. 45, no. 9, pp. 1348–1356, Sep. 1997.
[28] A. Petosa and A. Ittipiboon, "Dielectric resonator antennas: A historical review and the current state of the art," *IEEE Antennas Propag. Mag.*, vol. 52, no. 5, pp. 91–116, Oct. 2010.
[29] R. Chair, A. A. Kishk, and K.-F. Lee, "Comparative study on the mutual coupling between different sized cylindrical dielectric resonators antennas and circular microstrip patch antennas," *IEEE Trans. Antennas Propag.*, vol. 53, no. 3, pp. 1011–1019, Mar. 2005.
[30] A. Rashidian, L. Shafai, and D. M. Klymyshyn, "Compact wideband multimode dielectric resonator antennas fed with parallel standing strips," *IEEE Trans. Antennas Propag.*, vol. 60, no. 11, pp. 5021–5031, Nov. 2012.

MOHAMMAD ABEDIAN (Member, IEEE) received the B.Sc. degree in electrical and electronics engineering from the Babol Noshirvani University of Technology, Mazandaran, Iran, in 2008, and the M.Sc. and Ph.D. degrees in electrical–electronics and telecommunications engineering from University Technology Malaysia (UTM), Malaysia, in 2012 and 2015, respectively. From 2015 to 2016, he was a Research Fellow with the Wireless Communication Centre (WCC), UTM. From 2017 to 2018, he was a Research Fellow with the Iran University of Science and Technology (IUST), Iran. In 2019, he joined the Institute for Communication Systems (ICS), Home of the 5G and 6G Innovation Centre (5GIC and 6GIC), University of Surrey, Guildford, U.K., as a Research Fellow. His research interests include millimeter-wave antennas for 5G/6G applications, metasurfaces, dielectric resonator antennas, metamaterial antennas, and satellite array antennas.

MOHSEN KHALILY (Senior Member, IEEE) is currently a Senior Lecturer (an Associate Professor) in antennas and propagation and the Head of the Surface Electromagnetics Laboratory, Institute for Communication Systems, University of Surrey, U.K. He has published four book chapters and almost 160 academic articles in international peer-reviewed journals and conference proceedings and has been the principal investigator on research grants totaling more than $1.5 million in the field of surface electromagnetics. His research interests include surface electromagnetics, electromagnetic-engineered metasurfaces, phased arrays, THz metadevices, and mmWave and THz propagation. He is a Founding Member of the Industry Specification Group (ISG) on Reconfigurable Intelligent Surfaces (RIS) within the European Telecommunications Standards Institute (ETSI), where he serves as the Rapporteur for the work item on Implementation and Practical Considerations. He is also a fellow of the U.K. Higher Education Academy. He serves as an Associate Editor for IEEE Antennas and Wireless Propagation Letters, *Scientific Reports* (Nature), and IEEE Access.

PEI XIAO (Senior Member, IEEE) received the Ph.D. degree from the Chalmers University of Technology, Gothenburg, Sweden, in 2004. He is currently a Professor in wireless communications with the Institute for Communication Systems, Home of 5GIC and 6GIC, University of Surrey. He is also the Technical Manager of 5GIC/6GIC, leading the research team in the new physical layer work area, and coordinating/supervising research activities across all the work areas (https://www.surrey.ac.uk/institute-communication-systems/5g-6ginnovation-centre). Prior to this, he was with Newcastle University and Queen's University Belfast. He also held positions at Nokia Networks, Finland. He has published extensively in the fields of communication theory, RF and antenna design, and signal processing for wireless communications. He is an inventor on over 15 recent 5GIC patents addressing bottleneck problems in 5G systems.

FAN WANG received the B.S. and Ph.D. degrees in electronic engineering from Zhejiang University, Hangzhou, China. He joined Huawei Technologies Company Ltd., Shanghai, China, in 2008. From 2015 to 2016, he was with Huawei Technologies Sweden AB, Kista, Sweden. From 2019 to 2021, he was with Huawei Technologies (U.K.) Company Ltd., Reading, U.K. He has contributed to 3G/4G/5G physical layer standardization work and held numerous patents. His current research interests include B5G/6G wireless communication and massive machine-type communication.

RAHIM TAFAZOLLI (Senior Member, IEEE) is currently a Professor in mobile and personal communications and the Director of the Institute of Communication Systems (ICS) and the 5G and 6G Innovation Centre, University of Surrey. He has been active in research for over 30 years and published more than 1200 research papers. He has been a technical advisor to many mobile companies, and has lectured, chaired, and been invited as keynote speaker to a number of IEE and IEEE workshops and conferences. He served as the Chairperson for the EU Expert Group on Mobile Platform (e-mobility SRA), the Chairperson for the Post-IP working Group in e-mobility, and the past Chairperson of WG3 of WWRF. He is nationally and internationally known in the field of mobile communications. In May 2018, he was appointed as a Regius Professor in electronic engineering for recognition of his exceptional contributions to digital communications technologies over the past 30 years. He was elected as a fellow of the U.K. Royal Academy of Engineering, in 2020. He is a fellow of IET and the Wireless World Research Forum (WWRF).

AHMED A. KISHK (Life Fellow, IEEE) has been a Professor with Concordia University, Montréal, QC, Canada, since 2011, and the Tier 1 Canada Research Chair of Advanced Antenna Systems. He was a Distinguished Lecturer of the Antennas and Propagation Society (2013–2015). His research interests include electromagnetic applications. He has recently worked on millimeter-wave antennas for 5G/6G applications, analog beamforming networks, electromagnetic bandgap, phased array antennas, reflectors/transmitarray, and wearable antennas. In addition, he is a pioneer in dielectric resonator antennas, microstrip antennas, small antennas, microwave sensors, multi-function antennas, microwave circuits, and feeds for parabolic reflectors. He has published over 430-refereed journal articles and 520 international conference papers and 125 local and regional conference papers. He has coauthored four books and several chapters and was the editor of six books. He offered several short courses at international conferences.

He was a member of the AP-S AdCom (2013–2015) and the 2017 AP-S President. He is a member of several IEEE societies, such as the Antennas and Propagation Society, Microwave Theory and Techniques, Electromagnetic Compatability, Communications, Vehicular Technology Society, and Signal Processing. He is a Senior Member of the International Union of Radio Science, Commission B. In recognition, for contributions and continuous improvements to teaching and research to prepare students for future careers in antennas and microwave circuits, a fellow of Electromagnetic Academy, and a fellow of the Applied Computational Electromagnetics Society (ACES). He and his students received several awards. He won the 1995 and 2006 outstanding paper awards for papers published in the *Applied Computational Electromagnetic Society Journal*. He received the 1997 Outstanding Engineering Educator Award from the Memphis Section of the IEEE. He received the Outstanding Engineering Faculty Member, in 1998 and 2009, and the Faculty Research Award for Outstanding Research Performance, in 2001 and 2005. He received the Award of Distinguished Technical Communication for IEEE Antennas and Propagation Magazine's Entry, in 2001. He also received The Valued Contribution Award for an Outstanding Invited Presentation, ''EM Modeling of Surfaces with STOP or GO Characteristics—Artificial Magnetic Conductors and Soft and Hard Surfaces,'' from the Applied Computational Electromagnetic Society. He received the Microwave Theory and Techniques Society Microwave Prize, in 2004. He received the 2013 Chen-To-Tai Distinguished Educator Award from the IEEE Antennas and Propagation Society. He was an Editor of *IEEE Antennas and Propagation Magazine* (1993–2014) and the Editor-in-Chief of the ACES Journal from 1998 to 2001.